2018 IEEE-RAS 18th International Conference on Humanoid Robots (Humanoids)
Beijing, China, November 6-9, 2018

TWIMP: Two-Wheel Inverted Musculoskeletal Pendulum as a Learning Control Platform in the Real World with Environmental Physical Contact

Kento Kawaharazuka*,1, Tasuku Makabe*,1, Shogo Makino[1], Kei Tsuzuki[1], Yuya Nagamatsu[1], Yuki Asano[1]
Takuma Shirai[1], Fumihito Sugai[1], Kei Okada[1], Koji Kawasaki[2] and Masayuki Inaba[1]

***Abstract*— By the recent spread of machine learning in the robotics field, a humanoid that can act, perceive, and learn in the real world through contact with the environment needs to be developed. In this study, as one of the choices, we propose a novel humanoid TWIMP, which combines a human mimetic musculoskeletal upper limb with a two-wheel inverted pendulum. By combining the benefit of a musculoskeletal humanoid, which can achieve soft contact with the external environment, and the benefit of a two-wheel inverted pendulum with a small footprint and high mobility, we can easily investigate learning control systems in environments with contact and sudden impact. We reveal our whole concept and system details of TWIMP, and execute several preliminary experiments to show its potential ability.**

I. INTRODUCTION

In recent years, the spread of machine learning methods such as deep learning is rapid, and there have been big achievements in fields of image classification [1], sentence generation [2], etc. Also, machine learning is spreading in the robotics field, such as [3], [4], [5], and a humanoid that can act, perceive, and learn in the real world through contact with the environment needs to be developed.

Therefore, we propose a two-wheel inverted musculoskeletal pendulum TWIMP, as one of the choices to investigate learning control systems in the actual environment with contact and sudden impact. Our concept is a simple one that uses a tendon-driven musculoskeletal structure as an upper limb, and uses a two-wheel inverted pendulum as a lower limb. Because the musculoskeletal humanoid [6], [7], [8], [9] imitates human structures, it has many benefits such as the flexible spine, underactuated fingers, error recovery using redundant muscles, variable stiffness control using antagonism and nonlinear elastic feature of muscles, and joint torque control using muscle tension. Also, because the two-wheel inverted pendulum [10], [11] has high mobility and a small footprint, it can enter cluttered narrow spaces. By combining the benefits of these two, we can make learning control in the real world easier. In this study, we develop the two-wheel inverted musculoskeletal pendulum TWIMP, and conduct several preliminary experiments to show its potential ability.

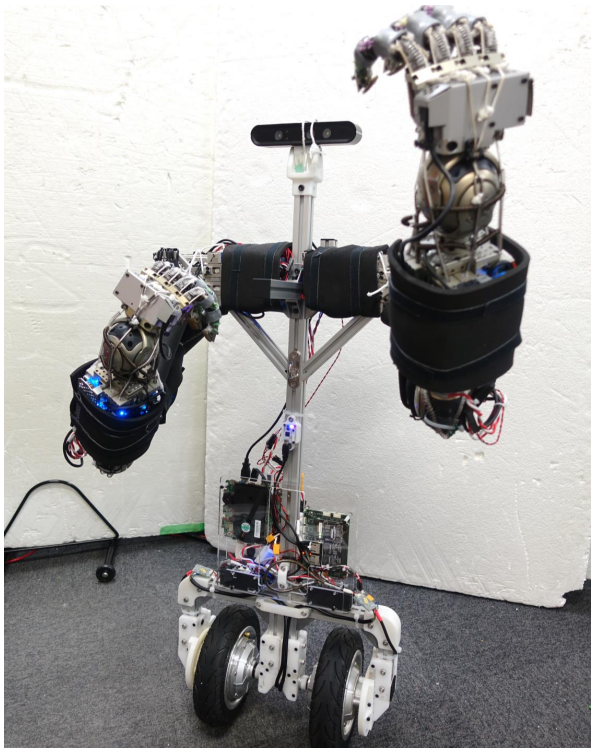

Fig. 1: Overview of TWIMP: Two-Wheel Inverted Musculoskeletal Pendulum

II. OUR APPROACH: MUSCULOSKELETAL HUMANOID WITH A TWO-WHEEL INVERTED PENDULUM

A. Overview of Our Proposed Approach

We propose a hybrid humanoid which has a musculoskeletal structure in the upper limb and a two-wheel inverted pendulum in the lower limb. The components of the musculoskeletal upper limb are fully modularized, and it can be constructed and reconstructed easily. The structure of the two-wheel inverted pendulum is constructed using a generic aluminum frame as with the musculoskeletal upper limb, and the modification of the link lengths and rearrangement of links are easy. By combining the two, we construct a two-wheel inverted musculoskeletal pendulum TWIMP, which has high impact resistance due to the flexible body structure

* K. Kawaharazuka and T. Makabe contributed equally to this work.
[1] The authors are with the Department of Mechano-Informatics, Graduate School of Information Science and Technology, The University of Tokyo, 7-3-1 Hongo, Bunkyo-ku, Tokyo, 113-8656, Japan. [kawaharazuka, makabe, makino, tsuzuki, nagamatsu, asano, t_shirai, sugai, k-okada, inaba]@jsk.t.u-tokyo.ac.jp
[2] The author is associated with TOYOTA MOTOR CORPORATION. koji_kawasaki@mail.toyota.co.jp

and high mobility, and which can be reconstructed according to the needs.

We control TWIMP using the general state feedback method with the optimal regulator, and add a control scheme to modify the upper body posture depending on the movements of the upper limb. We control the musculoskeletal upper limb using self-body image [12], [13] and joint torque control considering muscle tension [14].

We conduct basic movement, manipulation, and impact resistance experiments to show the potential ability of TWIMP, and discuss its control problems and its next generation design with a spine and tail.

B. Related Works and Our Contribution

We will discuss the related works regarding musculoskeletal humanoids, two-wheel inverted pendulums, and robots combining wheels and manipulators, separately.

So far, tendon-driven musculoskeletal humanoids such as Kenshiro [7] and Kengoro [9] have been developed. These robots aimed to mimic the musculoskeletal structures of human beings, and have underactuated structures, flexible muscle structures, etc. The controls of the upper limb such as variable stiffness control and muscle tension control have been developed to a practical level. However, regarding the movements of the lower limb, although controls such as the balancing control using muscle-ZMP [15] exist, precise control of the soft lower limb that supports the upper limb and walks stably is difficult, and the bipedal locomotion of the musculoskeletal humanoid has not been achieved yet. Therefore, manipulation with locomotion using the musculoskeletal humanoid has rarely been studied.

Regarding the two-wheel inverted pendulum, there are many studies such as [10] and [11], and the mobility is high. Also, it can move stably even on slopes. At the same time, trolly type robots can move more stably on level ground and no force is needed to stabilize the posture. Also, there are problems that both of them generally cannot get up after falling down.

Popular trolly type robots that combine wheels and manipulators are PR2 [16], Fetch [17], etc., and these play an active part in the robotics research field. However, because these robots cannot enter cluttered narrow spaces due to their big footprints, and cannot move stably on slopes, robots with not trollies but with wheeled inverted pendulums for locomotion have been developed. Handle of Boston Dynamics [18] has a wheel at each tip of two legs that move independantly, and can move stably using the multiple degrees of freedom on hilly landscapes that rise and fall. Emiew of HITACHI [19] has a human-like upper limb with dual arms and a head, and has a two-wheel inverted pendulum with high mobility, and it was popular as a human friendly navigation robot. However, all of these robots have rarely moved in situations with environmental physical contact, and they were developed with the weight on the mobility of the two-wheel inverted pendulum. Although UBot-5 [20] has two arms and a wheeled inverted pendulum in its small body and does learning control with environmental contact, we need to develop a life-sized humanoid that can be used more practically in the real world such as livelihood support and has more flexible arms with the ability to endure impacts due to large inertia.

Our contribution is that we propose a robot combining the musculoskeletal structure, which has high performance regarding soft contact with the environment and impact resistance, with the two-wheel inverted pendulum, which has a small footprint and high mobility, to be able to neutralize the disadvantages of these two and emphasize their benefits. This robot may be able to get up using the two wheels and flexible musculoskeletal dual arm, after falling down. Also, as a research platform of learning control systems, an easy design which can be constructed and reconstructed is desired, and this proposed robot is effective because it is designed using generic aluminum frames for almost all of the structures.

III. Design of TWIMP

In this section, we show the whole design of TWIMP. First, we explain the musculoskeletal dual arm and two-wheel inverted pendulum separately, and then explain TWIMP composed of these two.

A. Tendon-driven Musculoskeletal Dual Arm

The musculoskeletal dual arm is an extension of the single arm proposed in [21]. We show the detailed design in Fig.2. This arm has an easily reconfigurable structure composed of joint module, muscle module, and bone frame. Since a generic aluminum frame is used as the bone structure, we can construct the body structure freely and easily by combining the frames using brackets. The muscle module contains several sensors, which measure motor temperature, muscle length, and muscle tension. Since each joint module contains an IMU and potentiometers, we can obtain sensor information redundantly.

In addition, since the muscle is composed of a chemical fiber Dyneema and O-ring used as a nonlinear elastic element, it has a soft hardware structure. The nonlinear elastic element and antagonistic structure of the musculoskeletal humanoid enable variable stiffness control of the body joint.

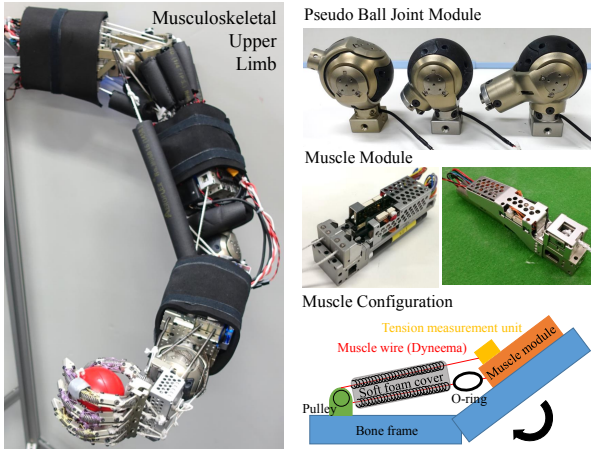

Fig. 2: Design of musculoskeletal upper limb

B. Two-wheel Inverted Pendulum

The detailed design of the two-wheel inverted pendulum is shown in Fig.3. We chose the wheel according to its output torque and easily configurable structure. So we used an in-wheel motor unit composed of a motor and wheel, and a generic aluminum frame as the bone structure, and achieved an easily reconfigurable simple wheel structure. TWIMP has rotary encoders outside of the in-wheel motor, and IMU at the trunk frame, and we control the posture, transition, and rotation of the inverted pendulum using the information from these sensors.

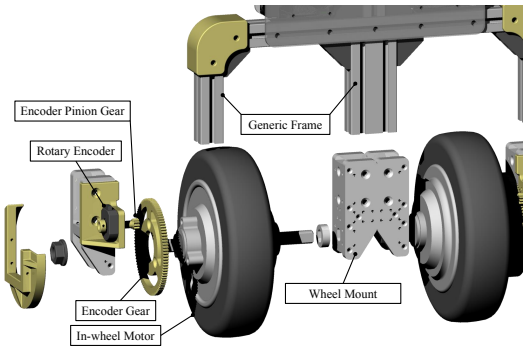

Fig. 3: Design of two-wheel inverted pendulum

C. Two-wheel Inverted Musculoskeletal Pendulum

The detailed design of TWIMP is shown in Fig.4. Since TWIMP is the combination of the upper limb in Subsection III-A and the lower limb in Subsection III-B using generic frames, we can change the link lengths easily. TWIMP has an AstraS camera as a RGB-D vision sensor on its head. The circuit configuration is shown in Fig.5. The circuit system of the high power humanoid JAXON [22] is used for the lower limb, and that of the musculoskeletal humanoid [21], with a space-saving characteristic, is used for the upper limb. To avoid damaging the circuits by its contact with the ground when TWIMP falls down, it has generic frames in the front and back of its chest frame.

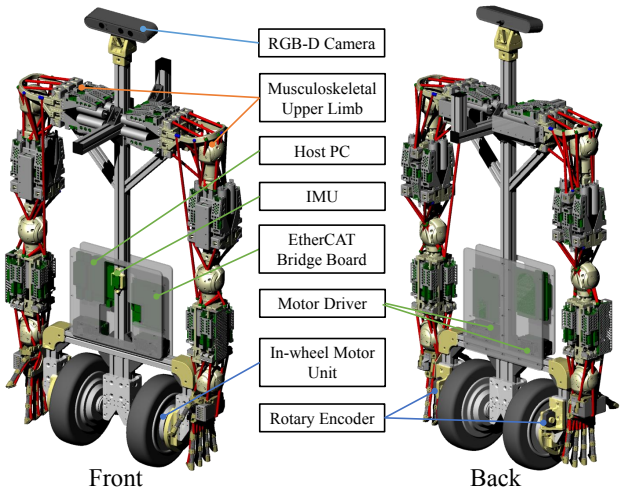

Fig. 4: Design of TWIMP

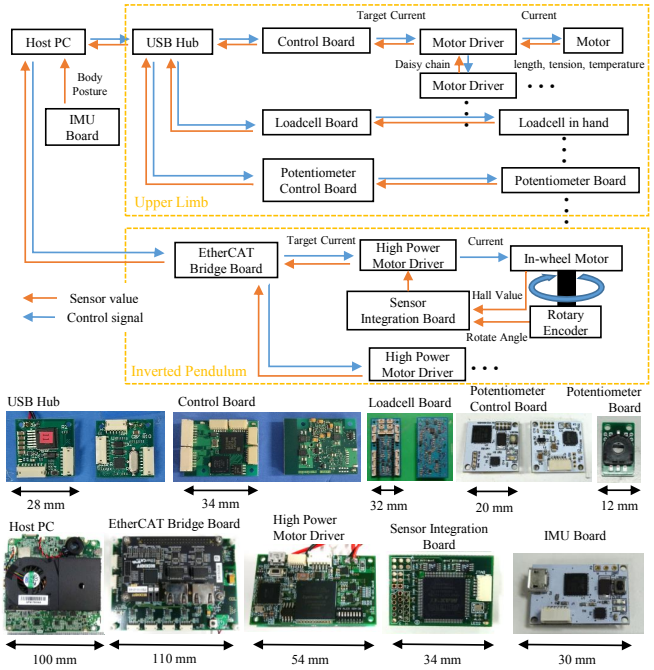

Fig. 5: Circuit configuration of TWIMP

IV. Control of TWIMP

In this section, we will explain the control system of TWIMP. First, we will explain the musculoskeletal dual arm and two-wheel inverted pendulum separately, and then, explain the integrated control system of TWIMP.

A. Control of Musculoskeletal Dual Arm

As the control of the musculoskeletal dual arm, (1) the control using the self-body image acquired with online training [13] and (2) the torque control using muscle tension [14] are possible. Concerning (1), we define the self-body image as below.

$$\boldsymbol{l}_{target} = \boldsymbol{f}_{ideal}(\boldsymbol{\xi}_{target}) + \boldsymbol{g}(\boldsymbol{\xi}_{target}, \boldsymbol{T}) \tag{1}$$

$\boldsymbol{l}_{target}$ is the target muscle lengths, $\boldsymbol{f}_{ideal}$ is the joint-muscle mapping in an ideal situation without external force, $\boldsymbol{\xi}_{target}$ is the target joint angles, $\boldsymbol{g}$ is the compensation term of the extension of muscles, and $\boldsymbol{T}$ is the current muscle tensions. In [13], this mapping is acquired by the initial training using the geometric model and online training using the actual robot. In this study, we trained the self-body image in advance, and conducted basic position control using Eq. 1.

Concerning (2), the target joint torques are calculated by proportional control, and the target muscle tensions are calculated to minimize the sum of the squares of muscle tensions as shown below.

$$\boldsymbol{\tau}_{ref} = K_j(\boldsymbol{\xi}_{ref} - \boldsymbol{\xi}) + \boldsymbol{\tau}_g(\boldsymbol{\xi}) \tag{2}$$

$$\text{minimize} \quad \boldsymbol{x}^T W \boldsymbol{x} \tag{3}$$

$$\text{subject to} \quad \boldsymbol{\tau}_{ref} = -G^T \boldsymbol{x} \tag{4}$$

$$\boldsymbol{x} \geq \boldsymbol{T}_{min} \tag{5}$$

τ_{ref} is the reference of joint torques, K_j is the gain of the proportional control, ξ_{ref} is the reference of joint angles, ξ is the current joint angles, τ_g is the torque of gravity compensation, x is the reference of muscle tensions (T_{ref}), W is the weight matrix, G is the muscle jacobian, and T_{min} is the minimum muscle tension.

B. Control of Two-wheel Inverted Pendulum

We use the general state feedback method as the control of the two-wheel inverted pendulum. As shown in Fig.6, we defined that θ is the slope of the base, ϕ is the rotation of the wheels from the base, m_w is the weight of the wheels, m_b is the weight of the base, I_w is the inertia of the wheels, I_b is the inertia of the base, R is the radius of the wheels, L is the distance between the center of mass of the base and wheels, τ is the torque of the wheels, and $x = \begin{bmatrix}\theta & \phi & \dot{\theta} & \dot{\phi}\end{bmatrix}^T$ is the state variable. Solving the lagrange equation, the state equation is shown as below.

$$E\dot{x} = A_0 x + B_0 \tau \tag{6}$$

$$\dot{x} = Ax + Bu \tag{7}$$

$$A = E^{-1}A_0, B = E^{-1}B_0, u = \tau \tag{8}$$

$$E = \begin{bmatrix} 1 & 0 & 0 & 0 \\ 0 & 1 & 0 & 0 \\ 0 & 0 & a+2b+c & a+b \\ 0 & 0 & a+b & a \end{bmatrix} \tag{9}$$

$$A_0 = \begin{bmatrix} 0 & 0 & 1 & 0 \\ 0 & 0 & 0 & 1 \\ d & 0 & 0 & 0 \\ 0 & 0 & 0 & 0 \end{bmatrix}, B_0 = \begin{bmatrix} 0 \\ 0 \\ 0 \\ 1 \end{bmatrix} \tag{10}$$

$$\begin{cases} a = (m_b + m_w)r_w^2 + I_w \\ b = m_b r_w l \\ c = m_b l^2 + I_b \\ d = m_b g l \end{cases} \tag{11}$$

The gain K of the feedback control $u = -Kx$ is calculated using the Ricatti equation by applying the optimal regulator to this state equation. The transitional direction is controlled by changing ϕ to $\phi_{ref} - \phi$. The rotational direction ψ is controlled with the proportional control, which adds the reversed torque calculated by multiplying the coefficient to the difference between the current and reference values to the left and right wheels as shown below, assuming that the influence to θ, ϕ is not large.

$$u_l = u_l - K_\psi(\psi_{ref} - \psi) \tag{12}$$

$$u_r = u_r + K_\psi(\psi_{ref} - \psi) \tag{13}$$

K_ψ is the proportional gain, $u_{\{l,r\}}$ is each torque of the left and right wheel, and ψ_{ref} is the reference of the rotational direction.

The state of $\theta, \dot{\theta}, \phi, \dot{\phi}, \psi$ is obtained from the IMU placed on the base and encoders of the wheels. In addition, we set $Q = \begin{bmatrix}500.0 & 1.0 & 500.0 & 0.2\end{bmatrix}^T, R = \begin{bmatrix}0.0001\end{bmatrix}$ in the evaluation equation $J = \int (x^T Q x + u^T R u)$ of the optimal regulator, and so, the trackability of ϕ is small compared with θ because the stabilization of the posture is the most important.

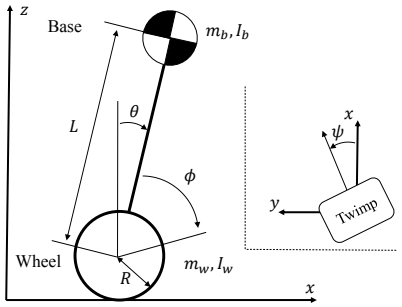

Fig. 6: Parameter configuration of two-wheel inverted pendulum

C. Control of TWIMP

The parameters of the state feedback are changed to a great extent due to the motion of the arms. Especially, the most important problem is the fluctuation of the center of mass, and it is necessary to deflect the body in order to keep the attitude when the arms are put forward. Therefore, the adaptation to the current center of mass is needed by changing θ_{ref} in response to ϕ, as shown below:

$$\theta_{ref} = \theta_{ref} + K_{adapt}\phi \tag{14}$$

where K_{adapt} is the proportional gain. This adaptation control has a dead zone, and θ_{ref} has to be changed gradually because sudden modification of θ_{ref} causes the robot to vibrate.

V. Preliminary Experiments

In this section, we will first explain the basic movement experiments using the lower and upper limb of TWIMP. Next, we will explain simple manipulation experiments using the musculoskeletal dual arm. Finally, we will explain several experiments regarding impact resistance.

A. Basic Movements of TWIMP

We conducted an experiment of translational and rotational movements with the arms fixed to the initial pose. First, we commanded $\phi_{ref} = 3.14$[rad] several times, making the robot go forward. After that, we commanded $\psi_{ref} = 3.14$[rad], making the robot turn around, and then, we commanded $\phi_{ref} = 3.14$[rad] again several times, making the robot go back to the original position. The result is shown in Fig.7. The values of ϕ and ψ increased to 3.14 [rad] immediately after the command, and correctly approached zero. In addition, the angle of attitude ϕ is in the range of $-0.05 \sim 0.05$[rad] during all motions.

Next, we conducted an experiment to stabilize the body while moving the arms. The result is shown in Fig.8. Due to the large movement in the center of mass when the pitch joints of the shoulders moved, ϕ moved greatly but converged correctly by changing θ_{ref} considering the value of ϕ in accordance with Eq. 14, though there is some offset. In addition, the robot moved stably with its arms raised by

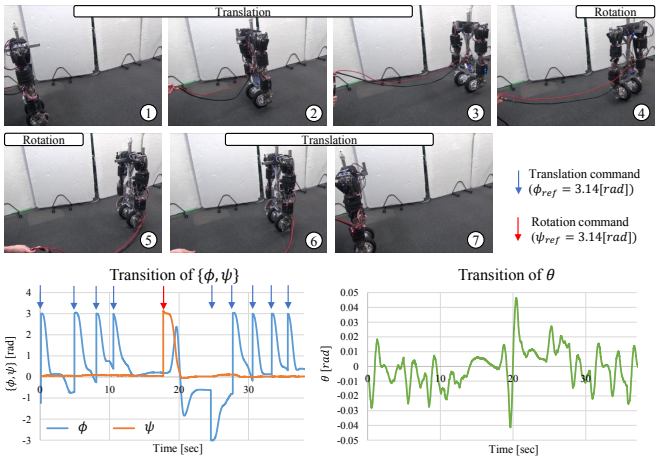

Fig. 7: The experiment of translational and rotational movements with the arms fixed to the initial pose.

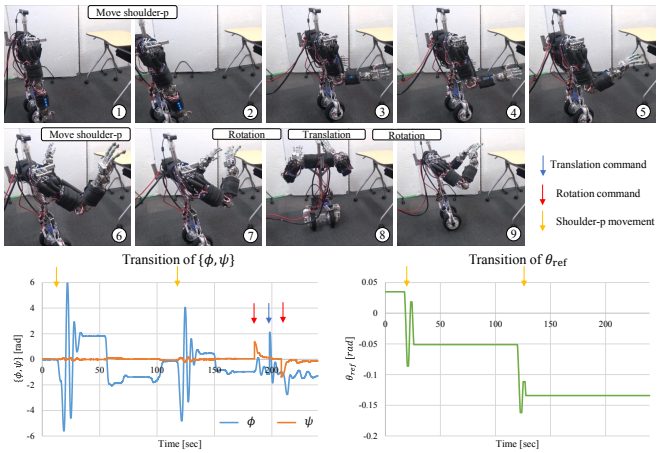

Fig. 8: Stabilization of TWIMP while moving its arms

converging ϕ and ψ when we sent translation and rotation commands.

B. Manipulation Experiments

First, we conducted the experiment of pushing a movable desk with casters. The arms were raised to the height of the desk. We commanded ϕ_{ref} to the front, and the attitude of the robot gradually tilted and pushed the desk by Eq. 14. The result is shown in Fig.9. θ_{ref} is gradually changed and the robot succeeded in pushing the desk.

Next, we conducted the experiment of holding a box with both hands and handing it to a person. The robot held a box placed on a desk with both arms, turned to a person, and released it when he held it. The result is shown in Fig.10. The robot succeeded in holding a box by pressing from both sides and in carrying the box to a person by commanding ϕ_{ref} and ψ_{ref}.

C. Stability from External Force

We investigated the stability against an impact by kicking the robot when the arms are in the initial position. The result is shown in Fig.11. The values of ϕ and ψ are converged

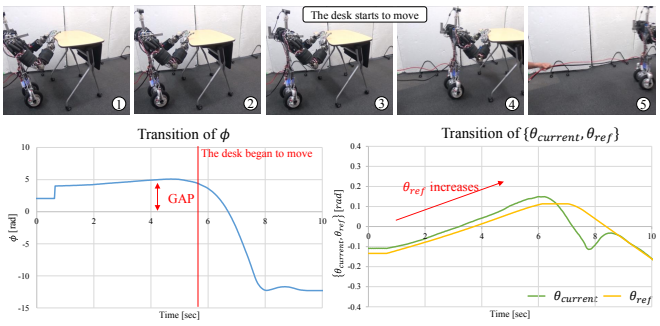

Fig. 9: The experiment of pushing a movable desk with casters.

in about 4 sec, though they are changed significantly at the time when we kicked the center of the robot.

Next, we investigated the stability with the arms raised when we hit the arms and base links. The result is shown in Fig.12. The robot was able to stabilize the attitude though ϕ, ψ, and θ were affected when we added short and long impact.

Finally, we investigated the resistance ability when an impact is added and the robot collides with a wall with the arms raised. The result is shown in Fig.13. ϕ and θ were changed at the moment of impact and changed rapidly when the robot collided with the wall. In addition, the muscle tension of the arms increased to more than twice the original value. However, the soft body structure absorbed the shock, and the tension and attitude returned to their original values.

VI. Discussion

We will start by considering the results of the conducted experiments.

First, while the robot moves stably in the transition and rotation experiment of Subsection V-A, we can see that the posture θ is changed greatly especially with the rotation of ψ. It seems that this is due to the fact that the rotation of ψ is not taken into account when considering the model of the state equation, though it is considered in several controllers such as [23]. Also, since we had to limit the speed of TWIMP, it is necessary to consider the translation ability and stability of the posture under a more dynamic system.

Second, during the movements of the arms in Subsection V-A, ϕ vibrates greatly at first and settles down in the end. This behavior of the robot will be improved by calculating the track of the center of mass using the model of the upper limb and feed forward control of θ_{ref} in addition to the control scheme of Subsection IV-C. However, we cannot decide if this is the best method, since the musculoskeletal structure is soft and there is a large error between the actual robot and its geometric model. In addition, we can consider installing a different control system such as the adaptive control. This discussion also occurs when considering the pushing desk motion in Subsection V-B, and we have to rethink the whole control scheme of this robot to manipulate objects stably.

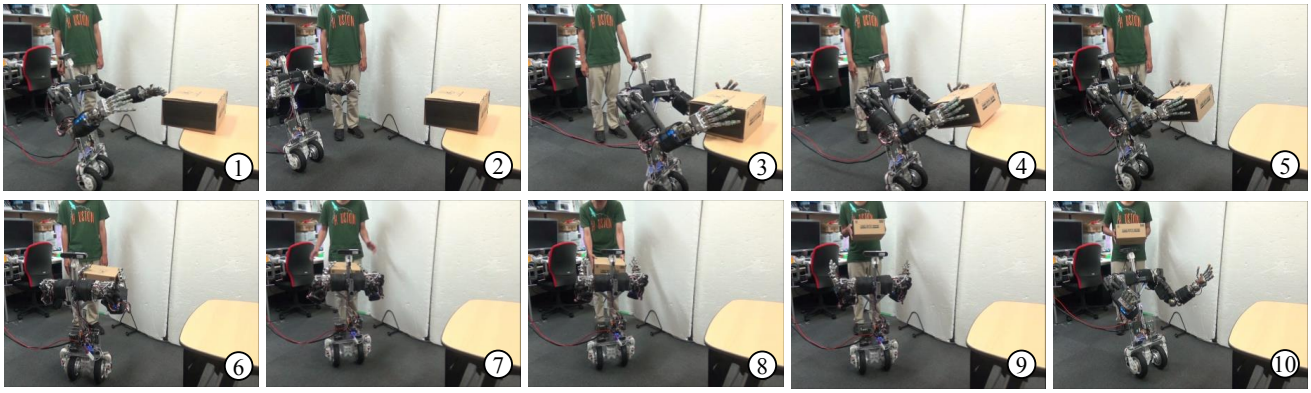

Fig. 10: The experiment of handing a box with both arms.

Third, we investigated stability resistance of TWIMP from impact in Subsection V-C, and these results seem to be due to the mobility and stability of the two-wheel inverted pendulum and the soft body structure of the musculoskeletal humanoid. However, although this robot has a high impact resistance ability and is not damaged when falling down, it has not succeeded in getting up yet.

Next, we will state future works of this study. We have discussed the problems of the present control methods, and we should examine motion generation using learning control methods. Learning control methods seem to be effective in not only solving the problems of modeling the soft body of the musculoskeletal humanoid, but also in moving in the real world with environmental contact. Since the musculoskeletal upper limb is soft and has tolerance to impact, it is rarely damaged when falling down and is suitable for motion learning in the real world. We would like to achieve advanced tasks such as livelihood support and care service. In addition, we should rethink the problems of robot hardware. Since TWIMP has to compensate for the change in the center of mass due to the arm movement by using only the base posture alteration, the whole robot posture changes according to the movement of the arms. We can solve the problem by adding either a spine or tail. The robot can change its posture freely and move more flexibly by modifying the trunk link to resemble the flexible spine structure, extending the design of the musculoskeletal upper limb. In addition, we suppose that a tail link will enable the stabilization of the robot body posture by changing the tail posture according to the arm movement, or by using the tail as a stand to support the body. As shown in this section, we believe that the two-wheel inverted musculoskeletal pendulum and its advancements will become the first step in the development of the learning robot, which is useful in the real world thanks to its soft hardware structure and mobility.

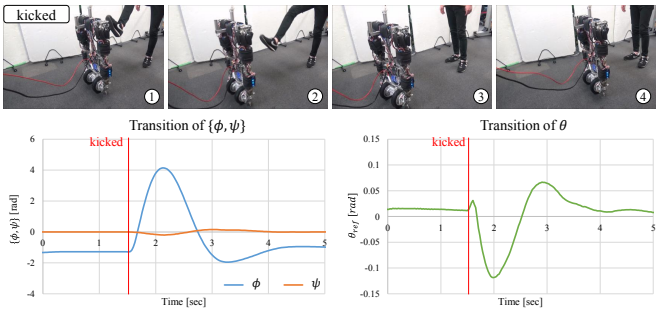

Fig. 11: The stability of TWIMP at the initial pose.

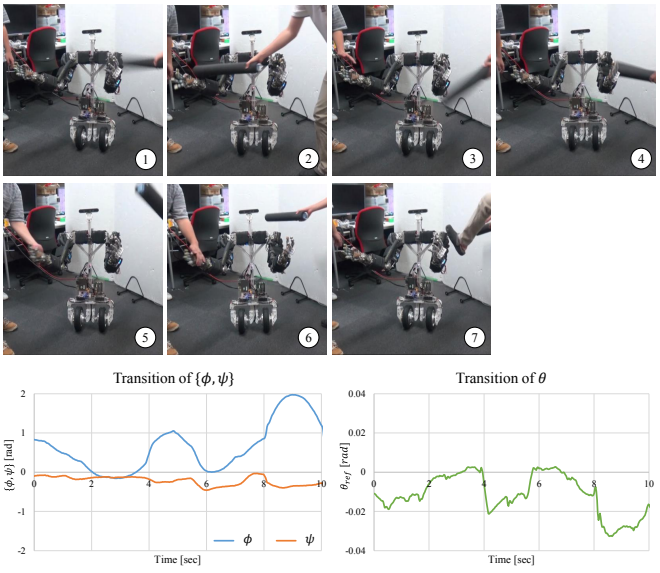

Fig. 12: The stability against the impact to the upper limbs.

VII. CONCLUSION

In this research, we proposed a two wheel inverted musculoskeletal pendulum: TWIMP, which is composed of a musculoskeletal upper limb and two-wheel inverted pendulum, as one of the platforms for researching learning control methods with environmental physical interactions in the real world. This robot has two advantages, which are the ability to contact the environment softly using the flexible structure of the musculoskeletal upper limb and variable stiffness mechanism, and the mobility of the two-wheel inverted pendulum which has a small footprint. We conducted several experiments concerning the ability of locomotion, manipulation, and durability using TWIMP, and we were able to show the potential ability by the combination of the soft upper body and the movable lower body. In future work,

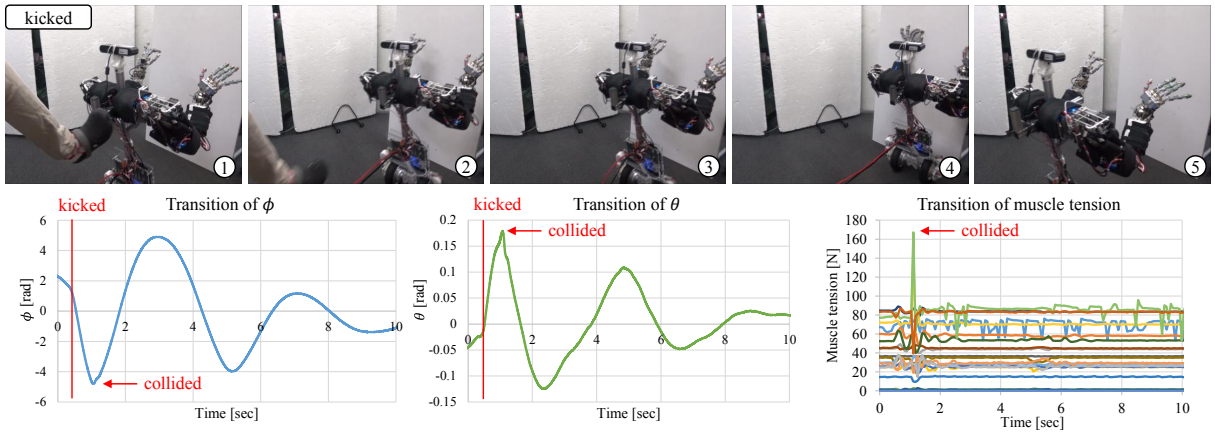

Fig. 13: The evaluation of the impact resistance in the experiment of collision with a wall.

we would like to study the learning control methods and advanced hardware design of TWIMP to make it useful in several situations such as livelihood support and care service.

ACKNOWLEDGEMENT

The authors would like to thank Yuka Moriya (Ochanomizu University) for proofreading this manuscript.

REFERENCES

[1] A. Krizhevsky, I. Sutskever, and G. E. Hinton, "Imagenet classification with deep convolutional neural networks," in *Advances in neural information processing systems*, 2012, pp. 1097–1105.

[2] A. Karpathy and L. Fei-Fei, "Deep visual-semantic alignments for generating image descriptions," in *Proceedings of the IEEE conference on computer vision and pattern recognition*, 2015, pp. 3128–3137.

[3] M. J. F. Zhang, J. Leitner, M. Milford, B. Upcroft, and C. Peter, "Towards vision-based deep reinforcement learning for robotic motion control," *arXiv preprint arXiv:1511.03791*, 2015.

[4] J. Tobin, R. Fong, A. Ray, J. Schneider, W. Zaremba, and P. Abbeel, "Domain randomization for transferring deep neural networks from simulation to the real world," in *Proceedings of the 2017 IEEE/RSJ International Conference on Intelligent Robots and Systems*. IEEE, 2017, pp. 23–30.

[5] S. Levine, P. Pastor, A. Krizhevsky, J. Ibarz, and Q. J. et al., "Learning hand-eye coordination for robotic grasping with deep learning and large-scale data collection," *The International Journal of Robotics Research*, vol. 37, no. 4-5, pp. 421–436, 2018.

[6] I. Mizuuchi, Y. Nakanishi, Y. Sodeyama, Y. Namiki, T. Nishino, N. Muramatsu, J. Urata, K. Hongo, T. Yoshikai, and M. Inaba, "An advanced musculoskeletal humanoid kojiro," in *Proceedings of the 2007 IEEE/RSJ International Conference on Intelligent Robots and Systems*, 2007, pp. 294–299.

[7] Y. Nakanishi, S. Ohta, T. Shirai, Y. Asano, T. Kozuki, Y. Kakehashi, H. Mizoguchi, T. Kurotobi, Y. Motegi, K. Sasabuchi, J. Urata, K. Okada, I. Mizuuchi, and M. Inaba, "Design approach of biologically-inspired musculoskeletal humanoids," *International Journal of Advanced Robotic Systems*, vol. 10, no. 4, p. 216, 2013.

[8] S. Wittmeier, C. Alessandro, N. Bascarevic, K. Dalamagkidis, D. Devereux, A. Diamond, M. Jäntsch, K. Jovanovic, R. Knight, H. G. Marques, P. Milosavljevic, B. Mitra, B. Svetozarevic, V. Potkonjak, R. Pfeifer, A. Knoll, and O. Holland, "Toward anthropomimetic robotics: Development, simulation, and control of a musculoskeletal torso," *Artificial Life*, vol. 19, no. 1, pp. 171–193, 2013.

[9] Y. Asano, T. Kozuki, S. Ookubo, M. Kawamura, S. Nakashima, T. Katayama, Y. Iori, H. Toshinori, K. Kawaharazuka, S. Makino, Y. Kakiuchi, K. Okada, and M. Inaba, "Human Mimetic Musculoskeletal Humanoid Kengoro toward Real World Physically Interactive Actions," in *Proceedings of the 2016 IEEE-RAS International Conference on Humanoid Robots*, 2016, pp. 876–883.

[10] K. Y. Kin, S. H. Kim, and Y. K. Kwak, "Dynamic analysis of a nonholonomic two-wheeled inverted pendulum robot," *Journal of Intelligent and Robotic Systems*, vol. 44, no. 1, pp. 25–46, 2005.

[11] S. Jeong and T. Takahashi, "Wheeled inverted pendulum type assistant robot: inverted mobile, standing, and sitting motions," in *Proceedings of the 2007 IEEE/RSJ International Conference on Intelligent Robots and Systems*. IEEE, 2007, pp. 1932–1937.

[12] K. Kawaharazuka, S. Makino, M. Kawamura, Y. Asano, K. Okada, and M. Inaba, "Online Learning of Joint-Muscle Mapping using Vision in Tendon-driven Musculoskeletal Humanoids," *IEEE Robotics and Automation Letters*, vol. 2, no. 4, pp. 2119–2126, 2018.

[13] K. Kawaharazuka, S. Makino, M. Kawamura, A. Fujii, Y. Asano, K. Okada, and M. Inaba, "Online Self-body Image Acquisition Considering Changes in Muscle Routes Caused by Softness of Body Tissue for Tendon-driven Musculoskeletal Humanoids," in *Proceedings of the 2018 IEEE/RSJ International Conference on Intelligent Robots and Systems (in press)*, 2018.

[14] M. Kawamura, S. Ookubo, Y. Asano, T. Kozuki, K. Okada, and M. Inaba, "A joint-space controller based on redundant muscle tension for multiple dof joints in musculoskeletal humanoids," in *Proceedings of the 2016 IEEE-RAS International Conference on Humanoid Robots*, 2016, pp. 814–819.

[15] Y. Asano, S. Nakashima, T. Kozuki, S. Ookubo, I. Yanokura, Y. Kakiuchi, K. Okada, and M. Inaba, "Human mimetic foot structure with multi-dofs and multi-sensors for musculoskeletal humanoid kengoro," in *Proceedings of the 2016 IEEE/RSJ International Conference on Intelligent Robots and Systems*. IEEE, 2016, pp. 2419–2424.

[16] "PR2 (Willow Garage)." http://www.willowgarage.com/pages/pr2/overview.

[17] "Fetch (Fetch Robotics)." https://fetchrobotics.com/.

[18] "Handle (Bostton Dynamics)." https://www.bostondynamics.com/handle.

[19] Y. Hosoda, S. Egawa, J. Tamamoto, K. Yamamoto, R. Nakamura, and M. Togami, "Basic design of human-symbiotic robot EMIEW," in *Proceedings of the 2006 IEEE/RSJ International Conference on Intelligent Robots and Systems*. IEEE, 2006, pp. 5079–5084.

[20] S. R. Kuindersma, R. A. Grupen, and A. G. Barto, "Variable risk control via stochastic optimization," *The International Journal of Robotics Research*, vol. 32, no. 7, pp. 806–825, 2013.

[21] K. Kawaharazuka, S. Makino, X. Chen, A. Fujii, M. Kawamura, T. Makabe, M. Onitsuka, Y. Asano, K. Okada, K. Kawasaki, and M. Inaba, "Design of a Musculoskeletal Upper Limb with Pseudo Ball Joint Modules for the Control of Redundant Nonlinear Elastic Elements," in *2017 JSME Conference on Robotics and Mechatronics*, 2017.

[22] K. Kojima, K. Karasawa, E. K. T. Kozuki, S. Yukizaki, S. Iwaishi, T. Ishikawa, R. Koyama, S. Noda, F. Sugai, *et al.*, "Development of life-sized high-power humanoid robot jaxon for real-world use," in *Proceedings of the 2015 IEEE-RAS International Conference on Humanoid Robots*. IEEE, 2015, pp. 838–843.

[23] J. Li, X. Gao, Q. Huang, and O. Matsumoto, "Controller design of a two-wheeled inverted pendulum mobile robot," in *Proceedings of the 2008 IEEE International Conference on Mechatronics and Automation*, 2008, pp. 7–12.